



|  |                |                    |                             |                |
|--|----------------|--------------------|-----------------------------|----------------|
| Document ID<br>1337317   | Version<br>1.0 | Status<br>Approved | Reg no                      | Page<br>1 (16) |
| Author<br>Rolf Sandström (Materials Science<br>and Engineering, KTH) |                |                    | Date<br>2012-03-14          |                |
| Reviewed by<br>Christina Lilja                                       |                |                    | Reviewed date<br>2012-04-13 |                |
| Approved by<br>Allan Hedin   |                |                    | Approved date<br>2012-04-13 |                |

# Analysis of a model for hydrogen bubble nucleation and growth in copper

## Abstract

Recently the paper "Hydrogen depth profile in phosphorus-doped, oxygen-free copper after cathodic charging" by Martinsson and Sandström has been submitted for publication. The paper describes experimental results as well as presenting a model. The experiments in the paper are based on maximum cathodic charging. The results are, however, of interest to apply to conditions with more modest charging, for example during corrosion. Since the model is entirely based on fundamental equations, it can be used to analyse what happens in new situations. In this report the effect of the charging intensity, the grain size, the critical nucleus size for hydrogen bubble formation as well as the charging time is analysed.

## 1 Basic assumptions in the model

This section gives a brief description of the model in Martinsson and Sandström's paper (referred to as the *paper* whereas this text is called the *report*).

The transport of hydrogen into the material is controlled by diffusion of hydrogen atoms, which satisfies the diffusion equation

$$\frac{dc_H}{dt} = D \frac{d^2 c_H}{dy^2} \quad (1)$$

where  $c_H$  is the hydrogen concentration in solid solution,  $t$  the time,  $D$  the diffusion constant for hydrogen and  $y$  the distance from the surface. The hydrogen flux to bubbles is also considered, where they form hydrogen molecules. The diffusion from bubbles back to the matrix is neglected due to low concentration of atomic hydrogen in the bubbles. The hydrogen flux  $J_H$  to a bubble is given by

$$J_H = D \nabla c_H = D \frac{c_H}{r} \quad (2)$$

where  $r$  is the bubble radius. This inflow gives rise to growth of the bubbles

$$\frac{dr}{dt} = \frac{D}{\rho_H} \frac{c_H}{r} \quad (3)$$

### Svensk Kärnbränslehantering AB

Swedish Nuclear Fuel and Waste Management Co  
PO Box 250, SE-101 24 Stockholm  
Visiting address Blekholmstorget 30  
Phone +46-8-459 84 00 Fax +46-8-579 386 10  
www.skb.se  
556175-2014 Seat Stockholm

$\rho_H$  is the density of hydrogen in the bubbles [ $\text{kg}/\text{m}^3$ ]. The bubble radius must exceed a critical value  $r_{\text{crit}}$  before it can start to grow

$$r_{\text{crit}} = \frac{2\gamma}{p} \quad (4)$$

where  $\gamma$  is the surface energy of the bubble and  $p$  the hydrogen pressure in it. The number of bubbles per unit volume  $n_V$ , is analysed below. With the help of conventional stereology,  $n_V$  can be related to the number of bubbles per unit area  $n_A$  provided the bubbles are approximately randomly distributed in the depth direction

$$n_A = 2rn_V \quad (5)$$

The change of  $\text{H}_2$ -concentration  $c_H$  due to the flux into the bubbles is, cf. eq. (3)

$$\frac{dc_H}{dt} = -4\pi r^2 n_V D \frac{c_H}{r} \quad (6)$$

Adding this contribution to (1) and using (5) gives the modified diffusion equation

$$\frac{dc_H}{dt} = D \frac{d^2 c_H}{dy^2} - 2\pi n_A D c_H \quad (7)$$

Eqs. (3) and (7) constitute a system for bubble radii and hydrogen content that can be solved numerically.

## 2 Influence of hydrogen inflow

The charging rate of hydrogen through the surface is assumed to be  $J = 1 \times 10^{-10} \text{ kg}/\text{m}^2/\text{s}$ . Since this parameter cannot be predicted, it has to be verified by checking that the total computed hydrogen content agrees with the experimental values. For the model values presented in the paper this is satisfied.  $J$  is the only parameter that is not determined independently of the modelling results.

The experiments presented in the paper are set up in such a way that the hydrogen charging is as large as possible. It can therefore be expected that under other charging conditions,  $J$  would be lower. In Figs. 1 to 5 it is illustrated how a change in  $J$  would affect the modelling results

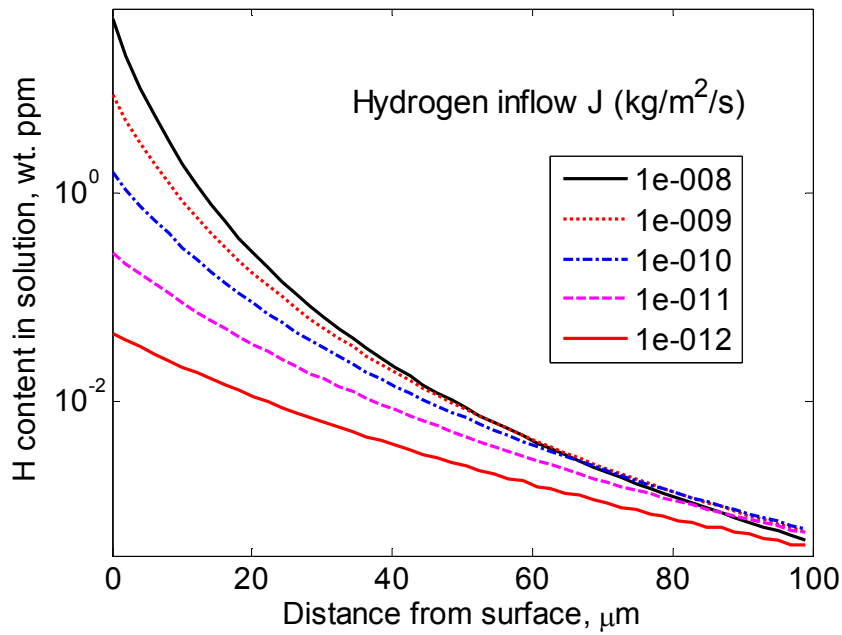


Fig. 1. Hydrogen content in solid solution as a function of distance from the surface for five levels of hydrogen inflow at the surface.

In Fig. 1 it can be seen that the inflow influences the amount of (atomic) hydrogen in solution in particular at the surface, but the variation there is not quite in proportion to the inflow. At greater depth the amount is fairly independent of the inflow.

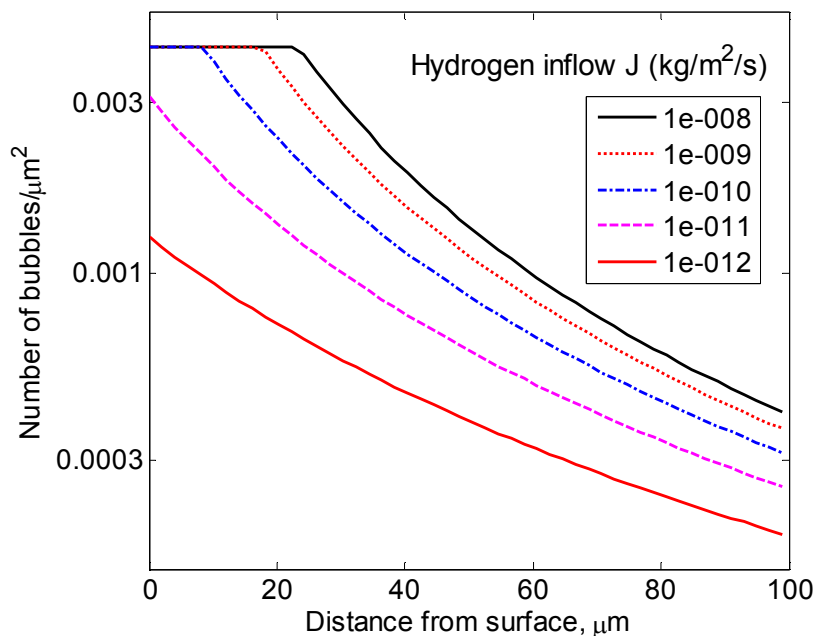


Fig. 2. Number of hydrogen bubbles as a function of distance from the surface for five levels of hydrogen inflow at the surface.

In Fig. 2 the predicted number of bubbles as a function of distance from the surface is shown. The variation between the inflow levels is largest at the surface.

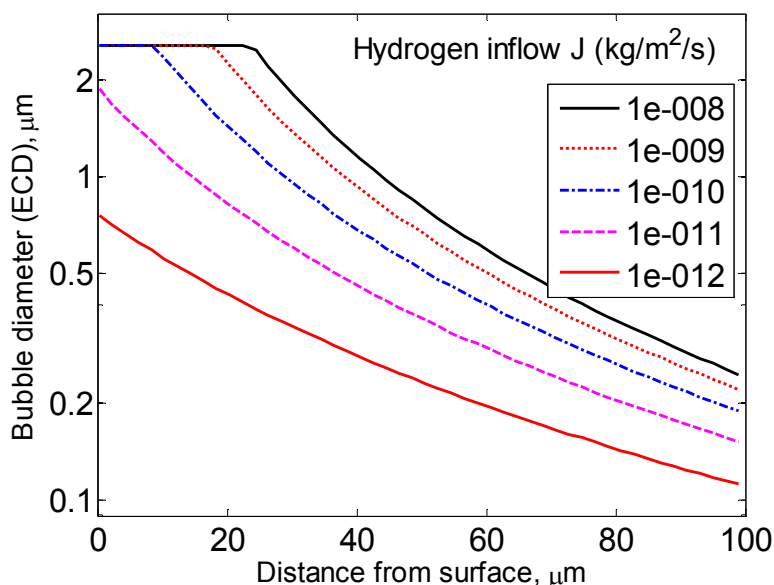


Fig. 3. The diameter of bubbles as a function of distance from the surface for five levels of hydrogen inflow at the surface.

The bubble diameter versus depth is illustrated in Fig. 3. Its relative variation with hydrogen inflow is very close to that of the number of bubbles in Fig. 2. Cut-off for the bubble diameter and the number of bubbles is introduced in Figs. 2 and 3. The reason for the cut-off is described below and in section 3.

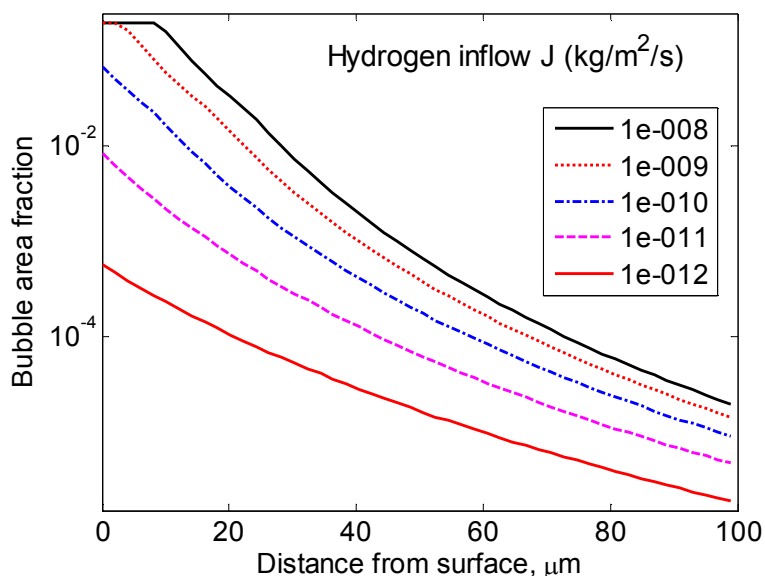


Fig. 4. Area fraction of bubbles as a function of distance from the surface for five levels of hydrogen inflow at the surface.

The bubble area fraction  $f_A$  can be expressed as

$$f_A = \pi r^2 n_A \tag{8}$$

This quantity is illustrated in Fig. 4. For inflows  $\geq 1 \times 10^{-10}$  kg/m<sup>2</sup>/s, the area fraction reaches its maximum value close to the surface. In the paper it was shown that the bubbles become unstable if the distance between them is less than one bubble diameter. With the bubbles in a quadratic net, this gives  $f_{Amax} = \pi/16 \sim 0.2$ . This value has been used as a cut-off in Fig. 4.

The density of hydrogen  $\rho_H$  (kg/m<sup>3</sup>) in a bubble is

$$\rho_H = \frac{p_H}{p_{atm}} \rho_{Hatm} \tag{9}$$

where  $p_H = 400$  MPa is the hydrogen pressure in the bubbles,  $p_{atm} = 0.1$  MPa the atmospheric pressure, and  $\rho_{Hatm}$  the hydrogen density at atmospheric pressure. From the hydrogen pressure and the bubble area fraction, the molecular hydrogen content  $c_{Hmol}$  can be obtained

$$c_{Hmol} = f_A \frac{\rho_H}{\rho_{Cu}} \tag{10}$$

$\rho_{Cu} = 8960$  kg/m<sup>3</sup> is the density of copper. The main part of the hydrogen in the material is in the form of molecular hydrogen in the bubbles. This content is illustrated in Fig. 5 using eq. (10). Since the hydrogen pressure in the bubbles is assumed to be constant, Fig. 5 has precisely the same appearance as in Fig. 4. The cut-off introduced in Fig. 4 is also apparent in Fig. 5. For an inflow of  $1 \times 10^{-10}$  kg/m<sup>2</sup>/s, the experimental cut-off is about 2000 wt. ppm. This indicates that the real cut-off for  $f_A$  could be lower but that is not consistent with the observed distribution of bubbles.

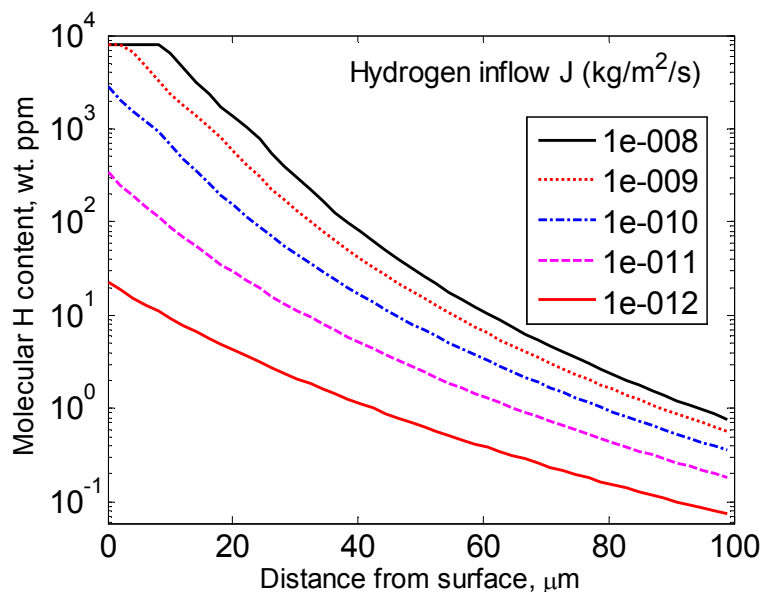


Fig. 5. Molecular hydrogen content in bubbles as a function of distance from the surface for five levels of hydrogen inflow at the surface.

The quantity in solid solution is negligible in comparison to the molecular content in the bubbles. The former is at least three orders of magnitude smaller, Fig. 1. The variation of the amount of molecular hydrogen with inflow is largest at the surface, Fig. 5. The variation is even somewhat larger than the change in the inflow. Deeper into the material the variation is smaller. This is logical since the total amount integrated over the depth should remain constant. This is also approximately the case, Table 1.

Table 1. Total amount of hydrogen

| Inflow of H (kg/m <sup>2</sup> /s)                                 | 1.00E-08 | 1.00E-09 | 1.00E-10 | 1.00E-11 | 1.00E-12 |
|--|----------|----------|----------|----------|----------|
| Nominal accumulated H content (kg/m <sup>2</sup> )                 | 0.018    | 0.0018   | 0.00018  | 1.8E-05  | 1.8E-05  |
| Accumulated H content in bubbles with cut-off (kg/m <sup>2</sup> ) | 0.0010   | 0.00064  | 0.00018  | 2.40E-05 | 2.4E-06  |

After three weeks ( $1.8 \times 10^6$  s) with an inflow of  $1 \times 10^{-10}$  kg/m<sup>2</sup>/s, the total nominal accumulated amount of hydrogen is 0.00018 kg/m<sup>2</sup>. This is the same value 0.00018 kg/m<sup>2</sup> obtained from integrating the content in the bubbles. The other values in Table 1 can be found in the same way. When the cut-off is taken into account the total amount of hydrogen is dramatically reduced for the largest inflows. Considering that the real cut-off can be even lower, this might explain why an inflow of  $1 \times 10^{-10}$  kg/m<sup>2</sup>/s seems to be close to the maximum possible one experimentally.

### 3 Influence of grain size

The grain size plays an important role since most of the hydrogen bubbles are formed at grain boundaries. Possible locations for nucleation of bubbles are grain corners, grain edges, and defects at the boundaries. For simplicity, the grains are assumed to consist of a set of cubes with the side  $d$ . Then the number of grain corners per unit volume  $n_{\text{corn}}$  is

$$n_{\text{corn}} = \frac{1}{d^3} \quad (11)$$

The length of grain edges per unit volume  $L_{\text{edge}}$  is

$$L_{\text{edge}} = \frac{12d}{4d^3} = \frac{3}{d^2} \quad (12)$$

This can be seen by considering that each cube has 12 edges and each edge belongs to 4 cubes. Since the critical diameter of a bubble is  $2 r_{\text{crit}}$ , cf. eq. (4), the maximum number of nuclei along an edge is  $d/(2 r_{\text{crit}})$  and the corresponding number per unit volume is

$$n_{\text{edge}} = \frac{L_{\text{edge}}}{2r_{\text{crit}}} = \frac{3}{2r_{\text{crit}}d^2} \quad (13)$$

As was shown in the paper, this expression describes well the number of observed bubbles as a function of distance from the surface. This does not mean that all the bubbles are positioned along the grain edges. This would also be impossible since the bubbles are much larger than  $r_{\text{crit}}$  after growth. Instead many bubbles can be found at defects at the grain sides.

With the help of eq. (5), the expression for  $n_{\text{edge}}$  (13) can be transferred to the number of bubbles per unit area  $n_A$

$$n_A = \frac{3r}{r_{\text{crit}}d^2} \quad (14)$$

This expression for  $n_A$  is illustrated in Fig. 6 as a function of grain size.

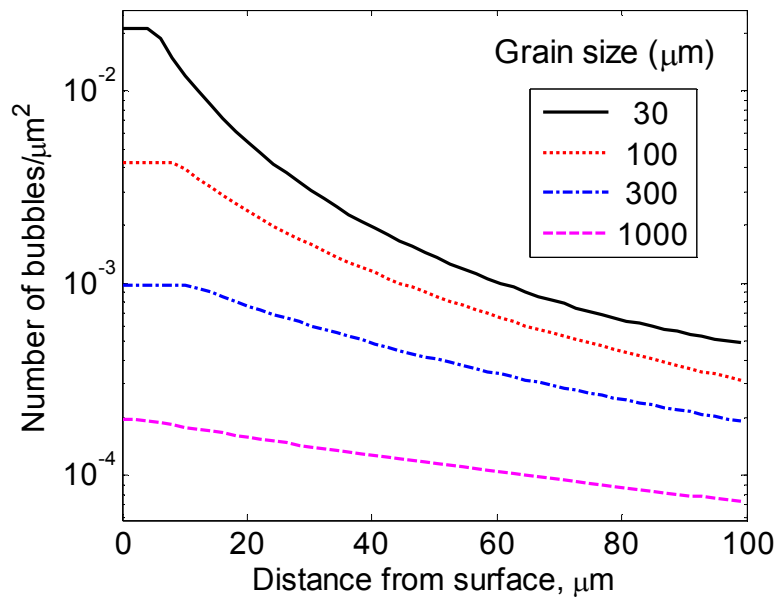


Fig. 6. Number of hydrogen bubbles as a function of distance from the surface for four grain sizes.

Close to the surface the grain size in eq. (14) is directly reflected in the number of bubbles in Fig. 6. The number of bubbles is proportional to  $1/d^2$ . Further away from the surface the influence of the grain size is much smaller.

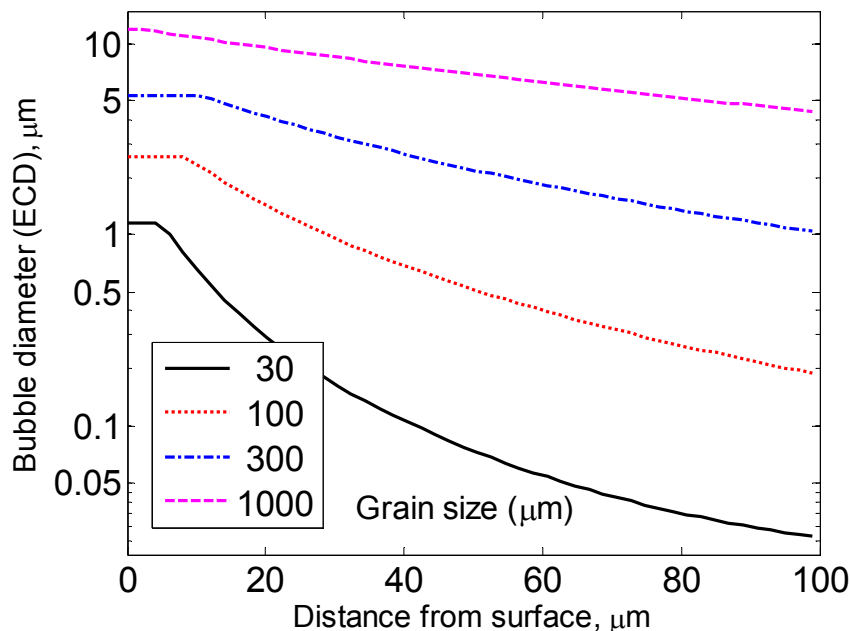


Fig. 7. Diameter of hydrogen bubbles as a function of distance from the surface for four grain sizes.

In Fig. 7, the bubble diameter is shown versus distance from the surface. In this case the largest variation as a function of grain size is inside the material. Close to the surface the both the number of bubbles and their diameter are high in the model, which would give rise to collapse of the bubbles.

This can be realised in the following way. From eq. (14) the distance between bubbles in the plane  $L_A$  can be obtained.

$$L_A = \frac{1}{\sqrt{n_A}} = \sqrt{\frac{r_{\text{crit}} d^2}{3r}} \tag{15}$$

This distance must be larger than twice the particle diameter to prevent collapse of the bubbles

$$\frac{L_A}{2r} = \sqrt{\frac{r_{\text{crit}} d^2}{3r}} \frac{1}{2r} = \sqrt{\frac{r_{\text{crit}} d^2}{12r^3}} \geq 2$$

which gives

$$r \leq r_{\text{max}} = \frac{r_{\text{crit}} d^2}{48} \tag{16}$$

The maximum bubble diameter that this gives is taken into account in Fig. 7 (and in Fig. 3) If this value is exceeded the bubbles will collapse and form a porous network where the hydrogen will leak out. This is another way of deriving the cut-off in connection with eq. (8).

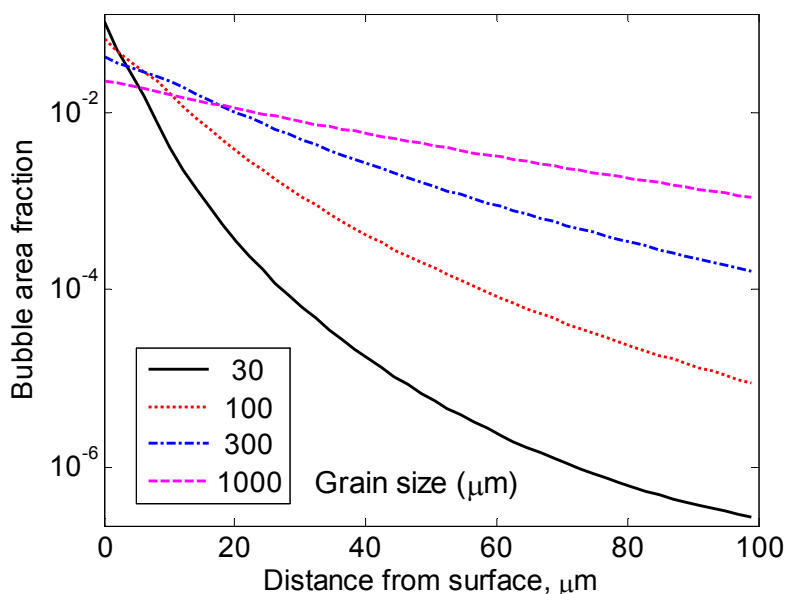


Fig. 8. Area fraction of hydrogen bubbles as a function of distance from the surface for four grain sizes.

In Fig. 8 the resulting bubble area fraction is shown for the four grain sizes. The grain size has a large influence inside the material. For smaller grain sizes the molecular hydrogen is concentrated to the surface area, whereas for the largest grain size significant hydrogen is found 0.1 mm from the surface.



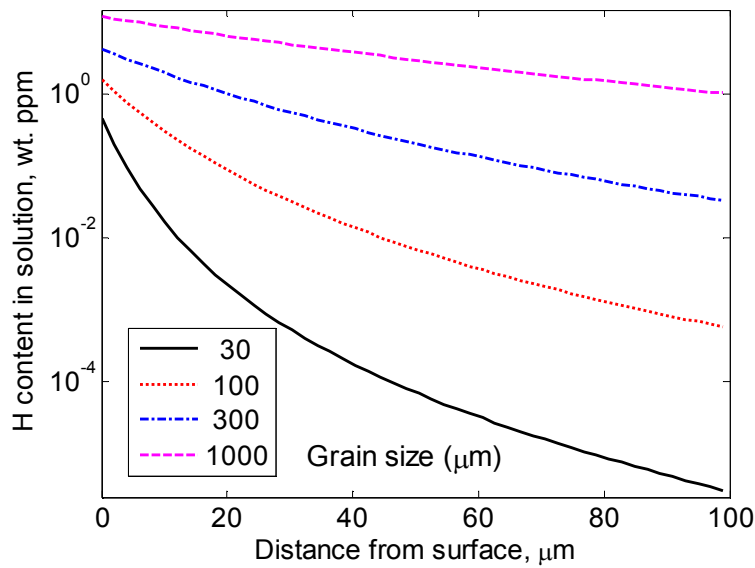


Fig. 9. Atomic hydrogen in solid solution as a function of distance from the surface for four grain sizes.

Fig. 9 illustrates the amount of hydrogen in solid solution. The grain size has quite a direct influence on this quantity. For the largest grain sizes the hydrogen has less opportunity to transfer to the bubbles simply due to the absence of bubble nuclei in the vicinity.

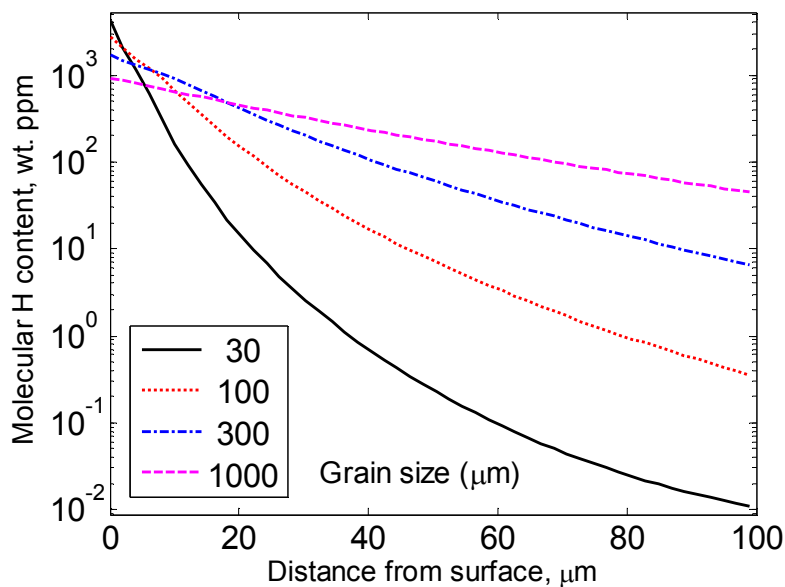


Fig. 10. Molecular hydrogen in bubbles as a function of distance from the surface for four grain sizes.

The amount of molecular hydrogen for different grain sizes is shown in Fig. 10. Since the molecular hydrogen is in the bubbles, Figs. 8 and 10 have precisely the same appearance. By integrating the profiles, the total amount of hydrogen in the material can be obtained. The values found are shown in Table 2.

Table 2. Total hydrogen content as a function of grain size

| Grain size ( $\mu\text{m}$ )   | 30      | 100     | 300     | 1000    |
|--|---------|---------|---------|---------|
| Accumulated H content in bubbles with cut-off ( $\text{kg}/\text{m}^2$ ) | 1.2E-04 | 1.8E-04 | 2.2E-04 | 2.0E-04 |

The nominal value for the uptake of hydrogen is  $1.8 \times 10^{-4} \text{ kg}/\text{m}^2$ , Table 1. The values in Table 2 are lower due to the collapse of bubbles close to the surface and the subsequent leakage. In the computations this is a result of the assumed cut-off in eq. (16).

## 4 Influence of the size of the critical bubble nuclei

The radius  $r_{\text{crit}}$  of the critical bubble nuclei is given in eq. (4). The value of the pressure  $p$  was determined to 400 MPa in the experiments by stress analysis of bubbles close to the surface in the paper. The pressure could be higher inside the material, since each bubble is surrounded by more copper. The pressure range 200 to 800 MPa is considered. For the surface energy experimental and theoretical values are found in the interval 1.79 to 2.24  $\text{J}/\text{m}^2$  (L. Vitos, A.V. Ruban, H.L. Skriver, J. Kolla, Surface Science 411 (1998) 186–202). A surface energy of 2.0  $\text{J}/\text{m}^2$  is used in the computations. Together with the observed pressure,  $r_{\text{crit}}$  is equal to 10 nm. An interval between 5 and 20 nm should cover possible values for  $r_{\text{crit}}$ .

The influence of the size of the critical nucleus is illustrated in Fig. 11. A factor of three variation is found at the surface but the variation inside the material is much smaller.

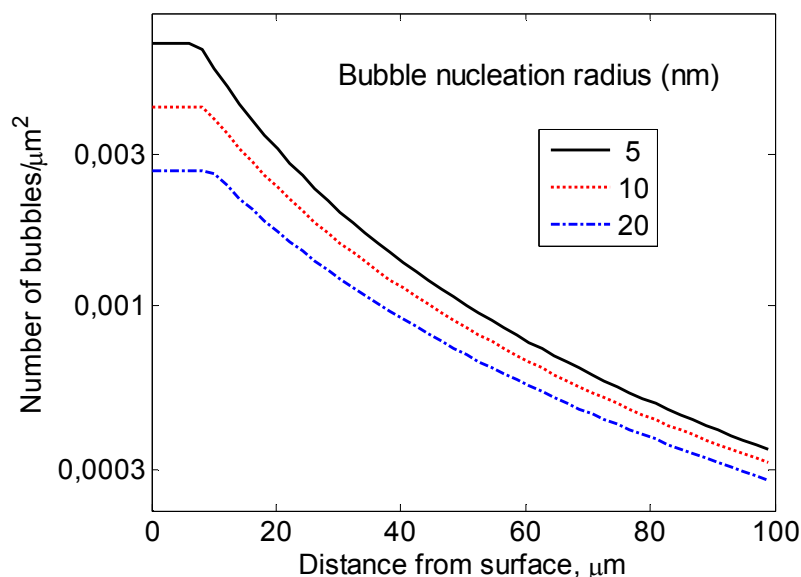


Fig. 11. Number of hydrogen bubbles as a function of distance from the surface for three radii of the critical nucleus.

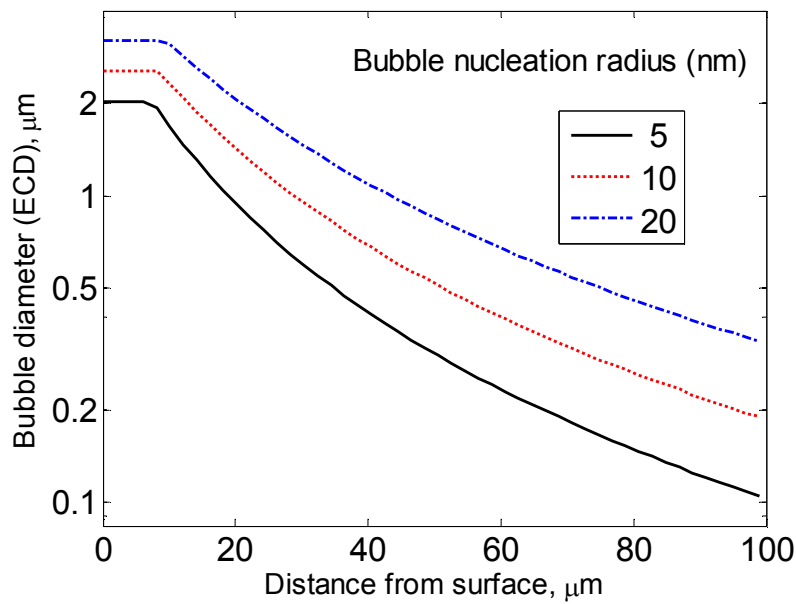


Fig. 12. Diameter of hydrogen bubbles as a function of distance from the surface for three radii of the critical nucleus.

For the bubble diameter the situation is reversed. The variation is largest inside the copper, Fig. 12.

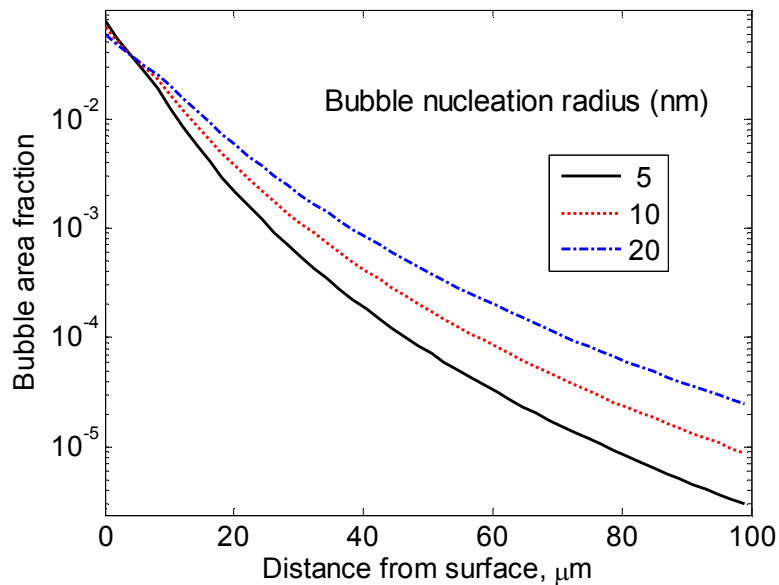


Fig. 13. Area fraction hydrogen bubbles as a function of distance from the surface for three radii of the critical nucleus.

Since the variation in the diameter is larger than for the number of bubbles, the changes in the diameters dominate the bubble area fraction, Fig. 13.

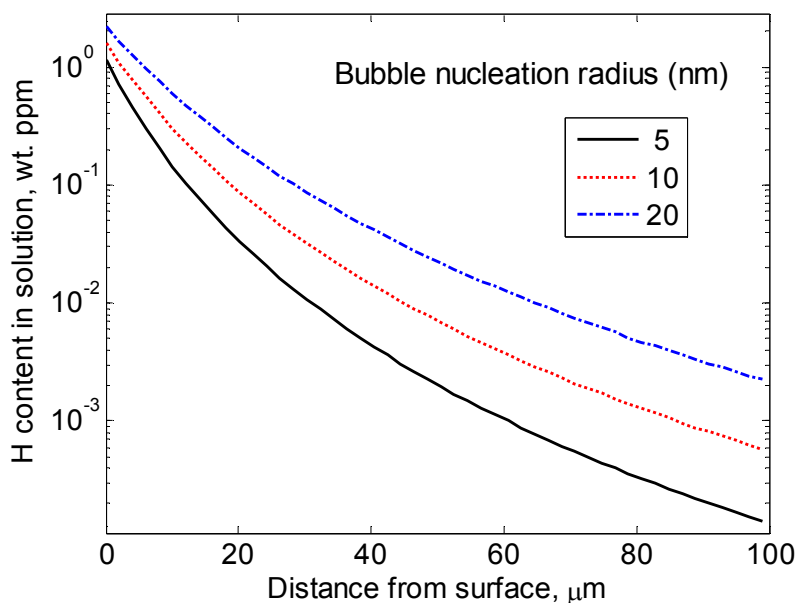


Fig. 14. Atomic hydrogen in solid solution as a function of distance from the surface for three radii of the critical nucleus.

For both the hydrogen in solid solution and in the bubbles, the influence of the nucleus size is more pronounced inside the material than at the surface, Figs. 14 and 15.

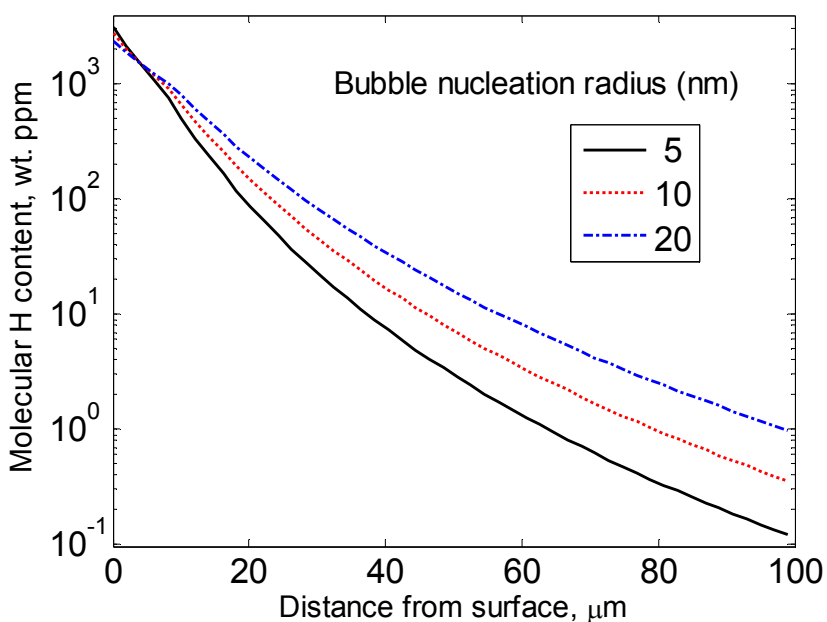


Fig. 15. Molecular hydrogen in bubbles as a function of distance from the surface for three radii of the critical nucleus.

## 5 Influence of charging time

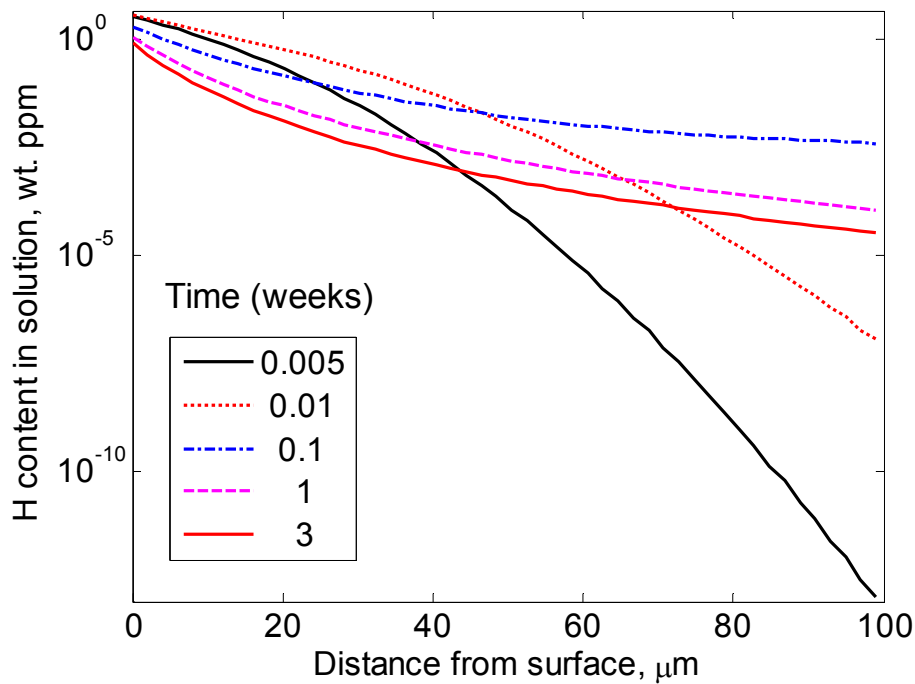


Fig. 16. Atomic hydrogen in solid solution as a function of distance from the surface for shorter charging times.

Fig. 16 illustrates how the amount of hydrogen in solid solution varies with shorter charging times. Initially the amount increases but already after 0.1 weeks a maximum has been reached and then a reduction is observed. The reason is that once the bubbles have reached a certain size the bubbles absorb hydrogen quickly from solid solution.

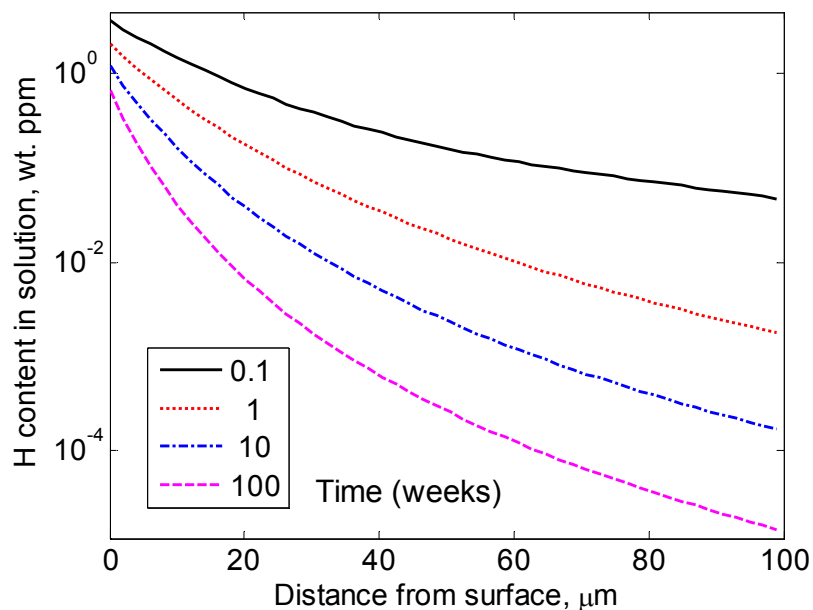


Fig. 17. Atomic hydrogen in solid solution as a function of distance from the surface for longer charging times.

For longer times there is a rapid decrease, Fig. 17. This also means that the rate of build up of the total amount of hydrogen is reduced, Fig. 18.

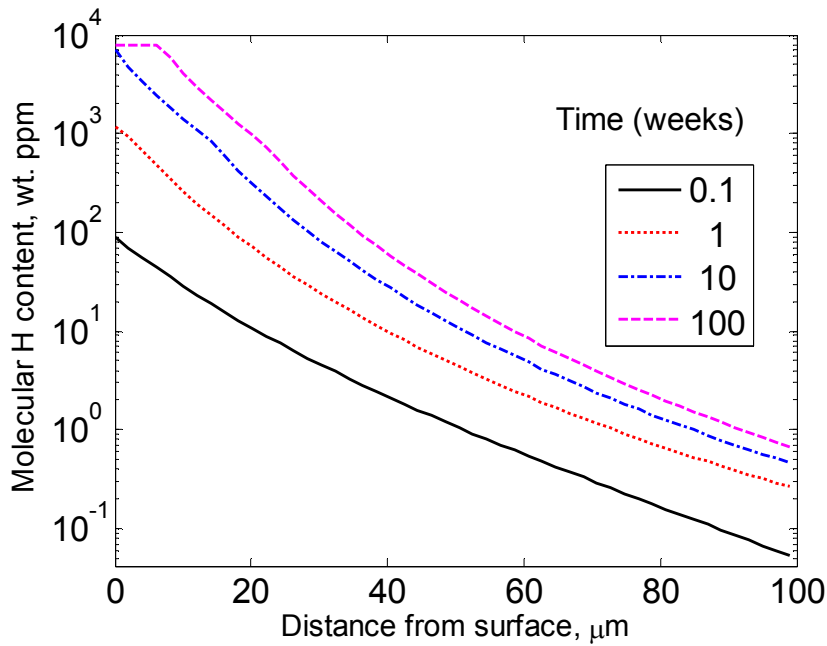


Fig. 18. Molecular hydrogen in bubbles as a function of distance from the surface for longer charging times.

The bubble diameter and number of bubbles show much the same behaviour, Figs. 19 and 20.

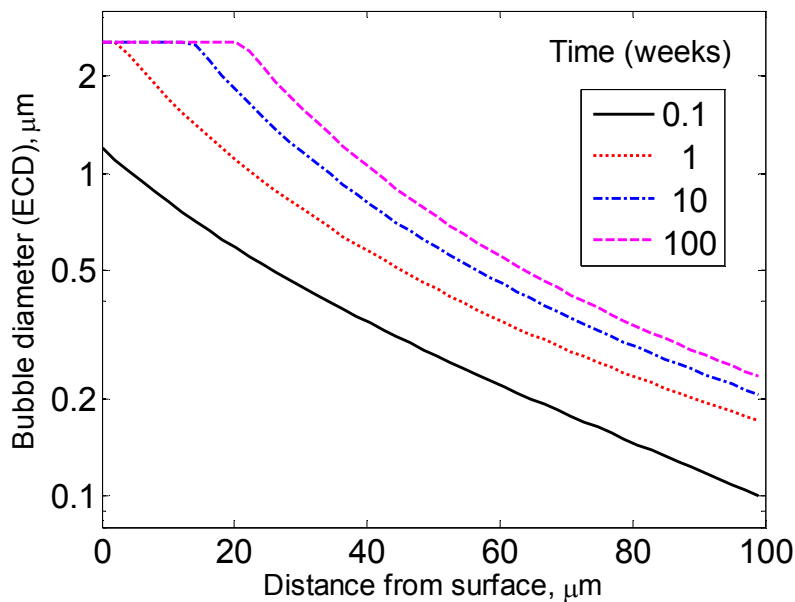


Fig. 19. Bubble diameter as a function of distance from the surface for longer charging times.

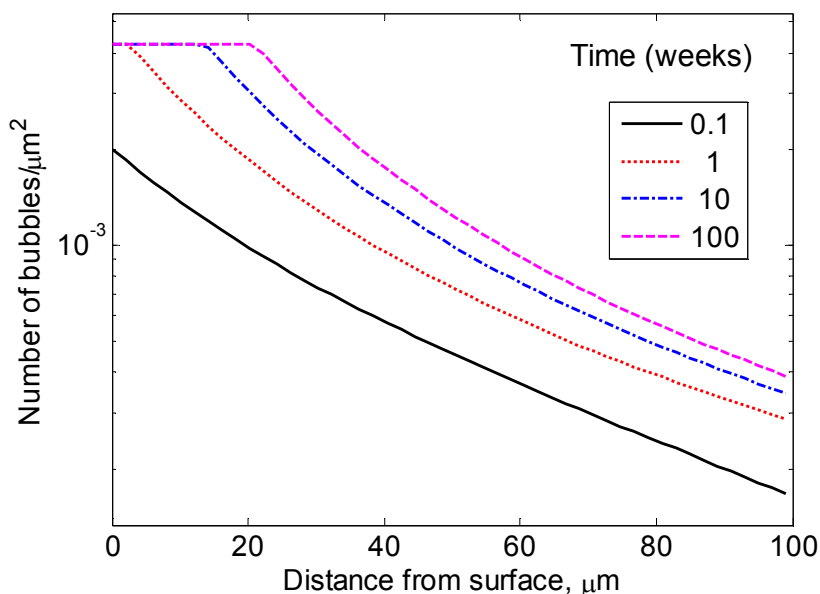


Fig. 20. Number of bubbles as a function of distance from the surface for longer charging times.

Most of the remaining inflow of hydrogen takes place close to the surface. However, at this position significant leakage of molecular hydrogen to the surface occurs. In addition outflow of atomic hydrogen by general diffusion takes place (S. Nakahara, *Acta Metallurgica*. 1988;36:1669-81). This implies that because of the reduced hydrogen built at longer times, a balance between inflow and outflow occurs and a stationary state is reached.

## Conclusions

- The experiments described in the paper were designed to give maximum charging. That this is closely the case is supported by the model. The computed inflow of hydrogen was  $1 \times 10^{-10}$  kg/m<sup>2</sup>/s. If a higher inflow is applied in the model the hydrogen bubbles near the surface get so close that they collapse due to the internal pressure. In this way open channels to the surface are formed, where molecular hydrogen can leak out.
- The hydrogen is stored in the material in two forms: atomic hydrogen in solid solution and molecular hydrogen in bubbles. During charging the amount of both forms shows a rapid exponential decrease with increasing distance from the surface. The amount of hydrogen is several orders of magnitude higher in the bubbles than in solid solution. After the charging has stopped, we have found experimentally that the amount of molecular hydrogen only drops slowly (unpublished results). The amount in solid solution, however, is reduced quickly by precipitation into the hydrogen bubbles forming molecular hydrogen.
- The critical radius for growth of a bubble depends on the surface energy in the bubble and the hydrogen pressure. The critical radius affects the hydrogen content inside the material.
- The computations and most experiments refer to a charging time of three weeks. For longer times the amount of hydrogen in solid solution is rapidly reduced. This means that the build up of the total hydrogen content is slowed down. Consider that an outflow of hydrogen takes place at a rate that is not decreasing. Eventually a stationary state will be reached with a balance between inflow and outflow implying that further build up of the hydrogen content is stopped.

- If the inflow is below  $1 \times 10^{-10}$  kg/m<sup>2</sup>/s which is expected to be the case during different types of corrosion, the amount of stored hydrogen is reduced in proportion. The reduction is largest close to the surface.
- From published tests on thin foils it is known that high hydrogen contents above 10 wt. ppm can give reduced ductility (Graebner, Okinaka, J. Appl. Phys. 60, 36 (1986)). From Swedish creep and tensile tests it is well established that copper with 0.6 wt. ppm has fully satisfactory ductility.
- For the analysed model cases the hydrogen content is below or close to 0.6 wt. ppm, 100 µm into the copper. The only exception is for large grain sizes. For 300 µm grain size the corresponding distance is about 200 µm. For a grain size of 1000 µm, the 0.6 wt. ppm level is reached at 400 µm distance from the surface. Although this result is not problematic, it is likely that other bubble nuclei inside the grains will become active. This will make the hydrogen profile steeper and shorten the distance to the 0.6 wt. ppm level. It should also be recalled that in the design premises for the canister a grain size of 360 µm or less is required.
- Consequently, only a very thin layer of material is exposed to a high hydrogen content. The mechanical properties of thick walled components are not influenced in a measureable way.